

# LFT/Hinf varying sampling control for Autonomous Underwater Vehicles

Emilie Roche, Olivier Sename, Daniel Simon

► **To cite this version:**

Emilie Roche, Olivier Sename, Daniel Simon. LFT/Hinf varying sampling control for Autonomous Underwater Vehicles. 4th IFAC Symposium on System, Structure and Control (SSSC 2010), Sep 2010, Ancona, Italy. 2010. <inria-00497049>

**HAL Id: inria-00497049**

**<https://hal.inria.fr/inria-00497049>**

Submitted on 2 Jul 2010

**HAL** is a multi-disciplinary open access archive for the deposit and dissemination of scientific research documents, whether they are published or not. The documents may come from teaching and research institutions in France or abroad, or from public or private research centers.

L'archive ouverte pluridisciplinaire **HAL**, est destinée au dépôt et à la diffusion de documents scientifiques de niveau recherche, publiés ou non, émanant des établissements d'enseignement et de recherche français ou étrangers, des laboratoires publics ou privés.

# LFT/ $\mathcal{H}_\infty$ varying sampling control for Autonomous Underwater Vehicles

E. Roche<sup>\*,\*\*</sup> O. Sename<sup>\*\*</sup> D. Simon<sup>\*</sup>

<sup>\*</sup> INRIA Grenoble Rhône-Alpes, NeCS team, Inovallée, Montbonnot, 38334 Saint-Ismier Cedex, France

Emilie.Roche@inrialpes.fr, Daniel.Simon@inrialpes.fr

<sup>\*\*</sup> GIPSA-lab - Department of Control Systems, ENSE<sup>3</sup>, rue de la Houille Blanche, BP 46, 38402 Saint Martin d'Hères Cedex, France  
olivier.sename@gipsa-lab.grenoble-inp.fr

## Abstract:

This paper deals with the robust control of an Autonomous Underwater Vehicle (AUV) subject to communication constraints. The aim is the design of a gain-scheduled varying sampling controller using non periodic measurements from ultrasonic sensors.

The contribution of this work lies in a new model formulation of varying sampling discrete-time systems using the Linear Fractional Transformation (LFT) representation.

This allows to design, in the LFT context, an  $\mathcal{H}_\infty$  controller whose matrices are scheduled w.r.t the varying control interval. Moreover the proposed design ensures a performance adaptation when the sampling interval varies. This methodology is developed for AUV and emphasizes important improvements compared with an  $\mathcal{H}_\infty$  discrete-time control with fixed sampling.

*Keywords:* AUV, Robust control, Gain scheduling, Varying Sampling

## 1. INTRODUCTION

In this paper the  $\mathcal{H}_\infty$  approach for LPV systems is applied to an Autonomous Underwater Vehicle (AUV) for altitude control. The use of AUV for the exploration of the seabed, and the control of these vehicles has been of large interest for researcher in the past two decades. Many different control laws were studied along the years : decoupling steering, diving, and speed control by PID (Jalving (1994)), coupled PID and anti-windup control (Miyamaoto et al. (2001)), sliding mode control (Healey and Lienard (1993); Salgado-Jimenez and Jouvencel (2003)) and  $\mathcal{H}_\infty$  control (Silvestre and Pascoal (2004); Feng and Allen (2004)).



Fig. 1. The Aster<sup>X</sup> AUV operated by Ifremer

The AUV considered in this paper is an Aster<sup>X</sup> like vehicle, developed by the Ifremer (French Research Institute for Exploitation of the Sea)<sup>1</sup>. In this preliminary study only motions in the vertical plane are considered: the

control of the yaw angle and speed are not taken into account.

The measurement of the altitude with respect to the sea floor is made using an ultrasonic sensor. Even if the measurement requests are made periodically, the signal flying time and the time at which the measures are received depend on the distance between the AUV and the sensor's target. This could be viewed as a delay in the reception of the measure, or as a need to apply the control samples in an asynchronous way. Another source of sampling intervals variations may come from sensors scheduling, needed to avoid cross-talking between several ultrasonic devices working in a close area. In this paper this time uncertainty is considered as a gain scheduling parameter for a LPV controller, as in Figure 2. Then the idea is to adapt the control interval with the distance between two samples, so that the controller only acts when a new measurement is available and processed. This approach allows for large measurement time variations because the controller is not only robust to a delay, but also scheduled according to the sampling interval variation.

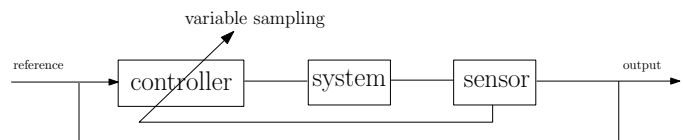


Fig. 2. Sensor acting on the sampling period of the controller

The control of underwater vehicles is made difficult by numerous non-linearities, due to cross-coupled dynamics and hydrodynamic forces subject to large uncertainties.

<sup>\*</sup> This work is supported by the FeedNetBack European project (FP7 IST 223866) and CONNECT ANR.

<sup>1</sup> <http://www.ifremer.fr/fleet/r&dprojets.htm>

Therefore robust control is necessary to safely perform autonomous missions : in this paper we use the ability of LPV based control to combine the performance specification in the  $\mathcal{H}_\infty$  framework, and the adaptation of the controller to parameters variations and uncertainties inside a specified range of values provided by the LPV approach.

In Robert et al. (2010) the LPV polytopic approach is used to design a control law with adaptation of the sampling period to account for the available computing resources for an inverted pendulum. In the present paper, the LPV approach relies on the LFT representation to compute the gain scheduled controller. Indeed the main drawback of the polytopic method could be the large number of LMIs to solve when the number of varying parameters increases. This is not the case in the LFT method and, as emphasized in Apkarian and Gahinet (1995), it leads to a LMI problem whose solution can directly be implemented. Moreover, this approach allows to consider in the same way varying parameters and uncertainties (adaptation to the parameters and robustness with respect to uncertainties).

The paper is organized as follows. Section 2 presents the non linear model of the AUV considered for the study and the model reduction for the vertical plane motion. Section 3 develops some theoretical background on model discretizing and on keeping the varying period as parameter, and also LPV/LFT control. Finally section 4 contains the control design and simulation results.

## 2. AUV MODELS

The model of the vehicle is directly inherited from Roche et al. (2009).

For the description of the vehicle behavior, we consider a 12 dimensional state vector :  $X = [\eta(6) \ \nu(6)]^T$ .

$\eta(6)$  is the position, in the inertial referential  $\mathcal{R}_0$ , describing the linear position  $\eta_1$  and the angular position  $\eta_2$ :  $\eta = [\eta_1 \ \eta_2]^T$  with  $\eta_1 = [x \ y \ z]^T$  and  $\eta_2 = [\phi \ \theta \ \psi]^T$  where  $x$ ,  $y$  and  $z$  are the positions of the vehicle, and  $\phi$ ,  $\theta$  and  $\psi$  are respectively the roll, pitch and yaw angles.

$\nu(6)$  represent the velocity vector, in the local referential  $\mathcal{R}$  (linked to the vehicle) describing the linear and angular velocities (first derivative of the position, considering the referential transform, see equation (2)) :  $\nu = [\nu_1 \ \nu_2]^T$  with  $\nu_1 = [u \ v \ w]^T$  and  $\nu_2 = [p \ q \ r]^T$

### 2.1 Non Linear Model

As given in Fossen (1994), Santos (1995), Jalving and Storkersen (1994), the physical model is given by the following dynamical equation:

$$M\dot{\nu} = G(\nu)\nu + D(\nu)\nu + \Gamma_g + \Gamma_u \quad (1)$$

$$\dot{\eta} = J_c(\eta_2)\nu \quad (2)$$

where:

-  $M$  is the mass matrix which represents the real mass of the vehicle augmented by the "water-added-mass" part,

-  $G(\nu)$  represents the action of Coriolis and centrifugal forces,

-  $D(\nu)$  is the matrix of hydrodynamics damping coefficients,

-  $\Gamma_g$  correspond to the gravity effort and hydrostatic forces,

-  $J_c(\eta_2)$  is the referential transform matrix from  $\mathcal{R}(C, xyz)$  towards  $\mathcal{R}_0(O, X_0Y_0Z_0)$ ,

-  $\Gamma_u$  represent the forces and moments due to the vehicle's actuators. The considered AUV has an axial propeller to control the velocity in Ox direction (forward force  $Q_c$ ) and 5 independent mobile fins :

- 2 horizontals fins in the front part of the vehicle (controlled with angles  $\beta_1$  and  $\beta'_1$ ).
- 1 vertical fin at the tail of the vehicle (controlled with angle  $\delta$ ).
- 2 fins at the tail of the vehicle (controlled with angles  $\beta_2$  and  $\beta'_2$ ) inclined with angle  $\pm\pi/3$  w.r.t the vertical fin.

The nonlinear model includes 12 state variables and 6 control inputs. For the computation of the controller, a linear model is proposed. The equilibrium point is chosen as  $[u \ v \ w \ p \ q \ r] = [1 \ 0 \ 0 \ 0 \ 0 \ 0]$  : all velocities are taken equal to 0, except the longitudinal velocity taken equal to 1m/s, the cruising speed chosen by the operator according to the payload requirements.

Tangential linearization around the chosen equilibrium point yields to a model of the form :

$$\begin{cases} \dot{x} = Ax(t) + Bu(t) \\ y = Cx(t) + Du(t) \end{cases}$$

where

- $x$  stand for the state :  $x = [x \ u \ y \ v \ z \ w \ \phi \ p \ \theta \ q \ \psi \ r]^T$
- $u$  for the control input  $u = [\beta_1 \ \beta'_1 \ \beta_2 \ \beta'_2 \ \delta_1 \ Q_c]^T$
- $y$  for the measured output (here only the altitude  $z$  is measured)

All the matrices  $A$ ,  $B$ ,  $C$  and  $D$  depend on the model parameters : hydrodynamical parameters, mass of the vehicle, dimension of fins... Note that most of these parameters are uncertain, and that here the control design is proposed for the nominal plant case only.

### 2.2 Model Reduction

The complete control of the vehicle is intricate due to the large size of the system. A usual solution is to separate the whole model into three different sub-models with reduced size. This allows for a "decoupling" control synthesis for the three directions  $Ox$ ,  $Oy$  and  $Oz$ .

To control the altitude  $z$ , the model is reduced to 4 state variables :  $z$ ,  $\theta$  (pitch angle) and the corresponding velocity  $w$  and  $q$ . For the actuation, only 4 fins are needed: the 2 horizontals fins in the front part of the vehicle ( $\beta_1$  and  $\beta'_1$ ) and the 2 oblique fins at the tail ( $\beta_2$  and  $\beta'_2$ ). Since the AUV has to stay in the vertical plan, both pairs of fins have to be actuated in the same way (with the same angle) so 2 control variable are chosen as:  $\beta_1 = \beta'_1$  and  $\beta_2 = \beta'_2$ .

*Remark* : In this paper we focus on the control of the altitude  $z$  with adaptation to the sampling period w.r.t. the measurement time, following the bottom referenced altitude control scenario. The other degrees of freedom are controlled using basic (i.e. constant sampling) feedbacks to keep the vehicle in the vertical plane with at the predefined forward velocity. Note that the model built for the control of the longitudinal speed  $u$  contains all the dynamics, but can only act on the propeller of the vehicle. To control the yaw angle  $\psi$ , the states variables are  $v$ ,  $\psi$  and  $r$ . The actions are the tree fins at the tail of the AUV (corresponding actions  $\delta$ ,  $\beta_2$  and  $\beta_2'$ ).

### 3. A LFT MODEL FOR VARYING SAMPLING PERIOD SYSTEMS

#### 3.1 Discrete time model with varying sampling period

This subsection describes the considered model, following the methodology in Robert et al. (2010).

Let us consider a continuous time state space representation of a system of the form :

$$G : \begin{cases} \dot{x} = Ax + Bu \\ y = Cx + Du \end{cases} \quad (3)$$

with  $A \in \mathcal{R}^{ns \times ns}$

The exact discretization of this system is describe in equation (5)

$$G_d : \begin{cases} x_{k+1} = A_d x_k + B_d u_k \\ y_k = C_d x_k + D_d u_k \end{cases} \quad (4)$$

with  $A_d \in \mathcal{R}^{ns \times ns}$  and

$$\begin{aligned} A_d &= e^{Ah} & B_d &= \int_0^h e^{A\tau} d\tau B \\ C_d &= C & D_d &= D \end{aligned} \quad (5)$$

The usual numerical method use the exponential of a matrix  $M$  :

$$\begin{pmatrix} A_d(h) & B_d(h) \\ 0 & I \end{pmatrix} = \exp \left( \begin{pmatrix} A & B \\ 0 & 0 \end{pmatrix} h \right) \quad (6)$$

The sampling period is assumed to belong to the interval  $[h_{min}, h_{max}]$  with  $h_{min} > 0$ , the sampling period is approximated around the nominal value  $h_0$  as :

$$h = h_0 + \delta \quad \text{with} \quad h_{min} - h_0 \leq \delta \leq h_{max} - h_0 \quad (7)$$

As explained in Robert et al. (2010) the equation (6) in this case becomes :

$$\begin{pmatrix} A_d(h) & B_d(h) \\ 0 & I \end{pmatrix} = \begin{pmatrix} A_{h_0} & B_{h_0} \\ 0 & I \end{pmatrix} \begin{pmatrix} A_\delta & B_\delta \\ 0 & I \end{pmatrix} \quad (8)$$

In case of an affine model in the variation of the sampling period  $\delta$  is needed, a Taylor series expansion of order  $k$  leads to :

$$A_\delta \approx I + \sum_{i=1}^k \frac{A^i}{i!} \delta^i \quad (9)$$

$$B_\delta \approx \sum_{i=1}^k \frac{A^{i-1} B}{i!} \delta^i \quad (10)$$

Finally the matrices of the discretized plant are :

$$\begin{aligned} A_d &= A_{h_0} A_\delta \\ B_d &= B_{h_0} + A_{h_0} B_\delta \end{aligned} \quad (11)$$

with  $A_d$  and  $B_d$  in an exact or approximate form, depending on the context.

#### 3.2 A new LFT Formulation for varying sampling systems

A LFT formulation is proposed in this section to express the system discrete time model by keeping the sampling period as a parameter (i.e. modeled as a system uncertainty).

First, an LPV/LFT model of a system, considering the sampling period as varying parameter is presented, based on the methodology developed in Robert (2007). The objective is to transform the system under the form described in Figure 3. The matrix  $\Delta$  represents the uncertainties depending on the sampling period  $h$ .

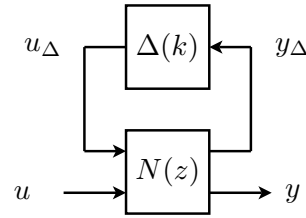


Fig. 3. System under LFT representation

Two cases are considered below in order to account for varying sampling period :

*Unstructured uncertainty case* From equations (11) two uncertainties blocks are derived :

$$\begin{aligned} \Delta_1 &= A_\delta - I \\ \Delta_2 &= A_{h_0} B_\delta \end{aligned} \quad (12)$$

The matrices of the discrete time system (4) are rewritten with these uncertainties :

$$\begin{cases} x_{k+1} = [A_{h_0} + A_{h_0} \underbrace{(A_\delta - I)}_{\Delta_1}] x_k + [B_{h_0} + \underbrace{A_{h_0} B_\delta}_{\Delta_2}] u \\ y = C_d x_k + D_d u \end{cases}$$

The system is transformed into the form described in Figure 3 by defining :

$$u_\Delta = [u_{\Delta_1}, u_{\Delta_2}]^T, \quad y_\Delta = [y_{\Delta_1}, y_{\Delta_2}]^T \quad \text{and} \quad \Delta = \begin{pmatrix} \Delta_1 & 0 \\ 0 & \Delta_2 \end{pmatrix}$$

Finally, the LFT form of the model with unstructured uncertainties (with no approximation) is as follows :

$$\begin{cases} x_{k+1} = \mathcal{A} x_k + \mathcal{B} \begin{pmatrix} u_\Delta \\ u \end{pmatrix} \\ \begin{pmatrix} y_\Delta \\ y \end{pmatrix} = \mathcal{C} x_k + \mathcal{D} \begin{pmatrix} u_\Delta \\ u \end{pmatrix} \end{cases} \quad (13)$$

$$\Delta = \begin{pmatrix} \Delta_1 & 0 \\ 0 & \Delta_2 \end{pmatrix}$$

$$\mathcal{A} = A_{h_0} \quad \mathcal{B} = (A_{h_0} \ I \ B_{h_0}) \quad (14)$$

$$\mathcal{C} = \begin{pmatrix} I \\ 0 \\ C_d \end{pmatrix} \quad \mathcal{D} = \begin{pmatrix} 0 & 0 & 0 \\ 0 & 0 & I \\ 0 & 0 & D_d \end{pmatrix}$$

The LPV/LFT model of the system is then given by the upper LFT interconnection

$$T_{u,y} = F_u(P(z), \Delta) = P_{22} + P_{21}\Delta(I - P_{11}\Delta)^{-1}P_{12} \quad (15)$$

This approach considers  $\Delta$  as a full block diagonal with full matrices  $\Delta_1$  and  $\Delta_2$ . However matrices  $\Delta_1$  and  $\Delta_2$  depend on a single parameter  $\delta$ , so this uncertainty definition may be too conservative.

*Structured uncertainty case* In order to reduce the conservatism the Taylor series expansion of order  $k$  (presented in (9) and (10)) for matrices  $A_\delta$  and  $B_\delta$  is used to obtain a structured uncertainty matrix.

$$\Delta_1 \approx A_\delta - I = \sum_{i=1}^k \frac{A^i}{i!} \delta^i$$

$$\approx A\delta \left( I + \frac{A\delta}{2} \left( I + \frac{A\delta}{3} \left( I + \dots \right) \right) \right) \quad (16)$$

$$\Delta_2 \approx A_{h_0} B \delta = A_{h_0} \sum_{i=1}^k \frac{A^i B}{i!} \delta^i$$

$$\approx A_{h_0} \left( I + \frac{A\delta}{2} \left( I + \frac{A\delta}{3} \left( I + \dots \right) \right) \right) B \delta \quad (17)$$

With this structure of uncertainty, the LFT representation of the system becomes (according to 3) :

$$\Delta = \delta I_{2 \times k \times n_s}$$

$$\mathcal{A} = A_{h_0} \quad \mathcal{B} = (\mathcal{B}_1 \ \mathcal{B}_2 \ B_{h_0}) \quad (18)$$

$$\mathcal{C} = \begin{pmatrix} \mathcal{C}_1 \\ \mathcal{C}_2 \\ C_d \end{pmatrix} \quad \mathcal{D} = \begin{pmatrix} \bar{\mathcal{D}} & 0 & 0 \\ 0 & \bar{\mathcal{D}} & \mathcal{D}_{2u} \\ 0 & 0 & D_d \end{pmatrix} \quad (19)$$

$$\mathcal{B}_1 = (A_a A \ 0_{n_s \times [n_s \times (k-1)]}) \quad \mathcal{B}_2 = (A_a \ 0_{n_s \times [n_s \times (k-1)]}) \quad (20)$$

$$\mathcal{C}_1 = \left. \begin{pmatrix} I_{n_s} \\ \vdots \\ I_{n_s} \end{pmatrix} \right\} k \text{ times}; \quad \mathcal{C}_2 = \left. \begin{pmatrix} 0_{n_s} \\ \vdots \\ 0_{n_s} \end{pmatrix} \right\} k \text{ times} \quad (21)$$

$$\bar{\mathcal{D}} = \begin{pmatrix} 0_{n_s} & \frac{A}{2} & \dots & 0_{n_s} \\ \vdots & \ddots & \ddots & \vdots \\ \vdots & \ddots & \ddots & \frac{A}{k} \\ 0_{n_s} & \dots & \dots & 0_{n_s} \end{pmatrix} \quad \mathcal{D}_{2u} = \begin{pmatrix} B \\ \vdots \\ B \end{pmatrix} \quad (22)$$

This allows to express the parameter block  $\Delta$  as a direct dependence on the varying sampling period  $\delta$ .

#### 4. BACKGROUND ON $\mathcal{H}_\infty$ / LFT CONTROL DESIGN

The objective is to get an LPV controller taking into account the set of parameter  $\Delta$  in the same way as the model, by a lower LFT interconnection :

$$T_{zw} = F_l(K, \Delta) := K_{11} + K_{12}K(I - K_{22}\Delta)^{-1}K_{21} \quad (23)$$

The LFT control scheme is presented in Figure 4, where the dependency on the parameters  $\Delta$  of the generalized plant  $P$  and of the controller  $K$  is described in an LFT form.

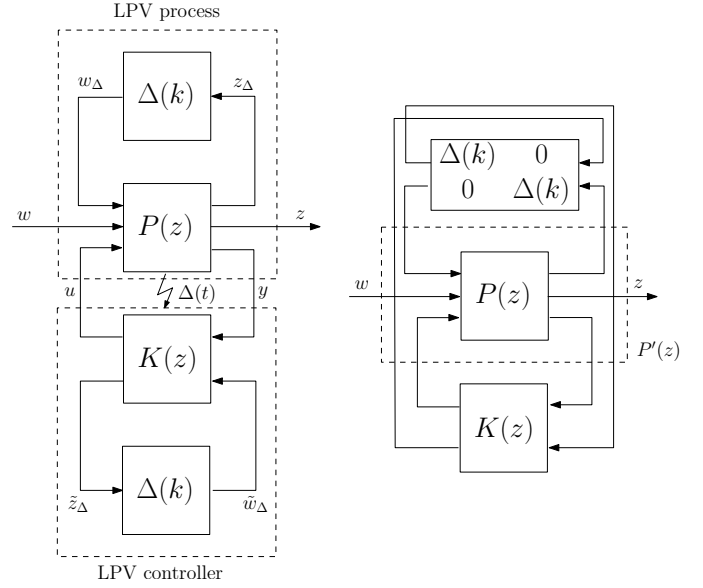


Fig. 4. LFT control scheme

The problem is now to find a discrete controller  $K$  for which the system described in Figure 4 is stable and respect some specifications defined by weighting functions set in the control loop ( $\mathcal{H}_\infty$  design).

The methodology used in this paper for the discrete-time controller synthesis is based on the  $\mathcal{H}_\infty$  framework, by the resolution of LMIs (derived from the bounded real Lemma), as described in Apkarian and Gahinet (1995) and Gauthier et al. (2007).

To reduce the conservatism due to the presence of uncertainties, the problem is reformulated using some scaling variables  $L_\Delta$ .

The solution of this problem relies on the bounded real Lemma, as follow :

*Lemma* Consider a parameter structure  $\Theta$ , the associated scaling set  $L_\Theta = \{L > 0 : L\Delta = \Delta L, \forall \Delta \in \Theta\}$ , and a discrete-time square transfer function  $T(z)$  of realization  $T(z) = D_{cl} + C_{cl}(zI - A_{cl})^{-1}B_{cl}$ , then the following statements are equivalent.

i)  $A_{cl}$  is stable and there exists  $L \in L_\Theta$  such that  $\|L^{1/2} (D_{cl} + C_{cl}(zI - A_{cl})^{-1}B_{cl}) L^{-1/2}\|_\infty < 1$ .

ii) There exist positive definite solutions  $X_{cl}$  and  $L \in L_\Theta$  to the matrix inequality

$$\begin{pmatrix} -X_{cl}^{-1} & A_{cl} & B_{cl} & 0 \\ A_{cl}^T & -X_{cl} & 0 & C_{cl}^T \\ B_{cl}^T & 0 & -L & D_{cl}^T \\ 0 & C_{cl} & D_{cl} & -L^{-1} \end{pmatrix} < 0 \quad (24)$$

The main result is as follows.

*Theorem 1.* Consider a discrete-time LPV plant  $P_\Delta(z)$  under LFT form. Let  $\mathcal{N}_r$  and  $\mathcal{N}_s$  denote bases of null spaces of  $(B_2^T, D_{\theta 2}^T, D_{12}^T, 0)$  and  $(C_2, D_{2\theta}, D_{21}, 0)$ , respectively.

With this notation, the gain-scheduled  $\mathcal{H}_\infty$  LFT control problem is solvable if and only if there exist pairs of symmetric matrices  $(R, S) \in \mathbb{R}^{n_a \times n_a}$  and  $(L_3, J_3) \in \mathbb{R}^{n_\theta \times n_\theta}$  and a scalar  $\gamma > 0$  such that

$$\mathcal{N}_r^T \begin{pmatrix} ARA^T - R + B_\theta J_3 B_\theta^T & & * \\ C_\theta RA^T + D_{\theta\theta} J_3 B_\theta^T & C_\theta RC_\theta^T + D_{\theta\theta} J_3 D_{\theta\theta}^T - J_3 & * \\ C_1 RA^T + D_{1\theta} J_3 B_\theta^T & C_1 RC_\theta^T + D_{1\theta} J_3 D_{\theta\theta}^T & * \\ B_1^T & D_{\theta 1}^T & * \\ & * & * \\ & * & * \\ C_1 RC_1^T + D_{1\theta} J_3 D_{1\theta}^T - \gamma I & * & * \\ D_{11}^T & * & -\gamma I \end{pmatrix} \mathcal{N}_r < 0$$

$$\mathcal{N}_s \begin{pmatrix} A^T SA - S + C_\theta^T L_3 C_\theta & & * \\ B_\theta^T SA + D_{\theta\theta}^T L_3 C_\theta & B_\theta^T SB_\theta + D_{\theta\theta}^T L_3 D_{\theta\theta} - L_3 & * \\ B_1^T SA + D_{\theta 1}^T L_3 C_\theta & B_1^T SB_\theta + D_{\theta 1}^T L_3 D_{\theta\theta} & * \\ C_1 & D_{1\theta} & * \\ & * & * \\ & * & * \\ B_1^T SB_1 + D_{\theta 1}^T L_3 D_{\theta 1} - \gamma I & * & * \\ D_{11} & * & -\gamma I \end{pmatrix} \mathcal{N}_s < 0$$

$$\begin{pmatrix} R & I \\ I & S \end{pmatrix} > 0$$

$$L_3 \Theta = \Theta L_3, J_3 \Theta = \Theta J_3, \begin{pmatrix} L_3 & I \\ I & J_3 \end{pmatrix} > 0$$

This LMI is then solved using Yalmip interface (Lofberg (2004)) and Sedumi solver (Sturm (1999)).

## 5. $\mathcal{H}_\infty$ CONTROL DESIGN FOR AUVS

### 5.1 LFT model of the AUV

An LPV/LFT model of the AUV considering the sampling period as varying parameter, using the methodology previously described is built. The Taylor series expansion described in equation (16) and (17) is made at order  $k = 2$ . Here the Bode diagram of this LPV/LFT system is presented on Figure 5, using the structured case uncertainties :

$$\Delta = \delta I_{2 \times k \times n_s} \quad (25)$$

According to the sampling period variation, this Bode Diagram shows a variation on the system gain and also on the bandwidth.

### 5.2 Structure and weighting function

The method is based on the  $\mathcal{H}_\infty$  control design. The first step is to choose a control structure and weighting functions that will be placed in the control loop for setting some specifications (response time in closed loop, tracking error...).

We choose the following classical structure, with :

- $W_e$  a weight on the tracking error, for fixing specifications on the controlled outputs  $y$  (here only the

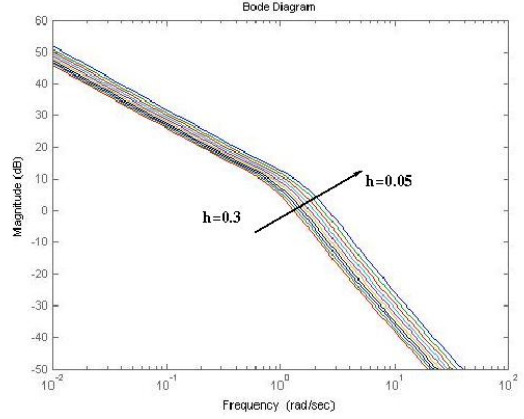


Fig. 5. Bode diagram of the system

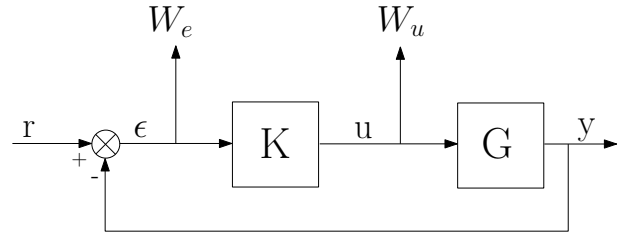


Fig. 6. Structure chosen for the control design

altitude  $z$  has to be controlled). The varying sampling period considered for the controller synthesis imposes a parametrized discretization of weights. This allows the adaptation of the performances with respect to the current sampling period, as explained in Robert et al. (2010). So  $W_e$  is defined with the following state space system, with the frequency  $f = 1/h$  :

$$\begin{cases} \dot{x} = (a \times f)x + (a \times f - b \times f)u \\ y = x + u \end{cases} \quad (26)$$

This weight is then discretized to obtain discrete-time representation :

$$W_d(z) : \begin{cases} x_{k+1} = A_d x_k + B_d u_k \\ y_k = x_k + u_k \end{cases} \quad (27)$$

$$\begin{cases} A_d = e^{afh} = e^a \\ B_d = (af)^{-1}(A_d - I)bf = a^{-1}(A_d - I)b \end{cases} \quad (28)$$

The simplification between  $h$  and  $f$  leads to discrete LTI representation of the weight.

The elements  $a$ , and  $b$  are chosen for obtaining :

- a good robustness margin.
- a tracking error less than 1%.
- a settling time of 5 seconds.
- $W_u$  is chosen to account for actuator limitations (all element where normalized, so we choose the identity matrix of size 4 for  $W_u$ ).

Then the augmented plant ( $P$  in Figure 4) is built containing the model of the system and the weighting functions.

### 5.3 LFT controller

A LPV/LFT controller is computed for the control of the altitude  $z$ , by considering the the previous structure and weights.

The interval of variation of the sampling period for the controller design is :  $h \in [0.05; 0.3]s$

Similarly to the Bode diagram of the system, the controller Bode diagram varies according to the sampling period, as seen in Figure 7. The sampling period clearly affects the controller bandwidth, this in accordance with the system bandwidth variation.

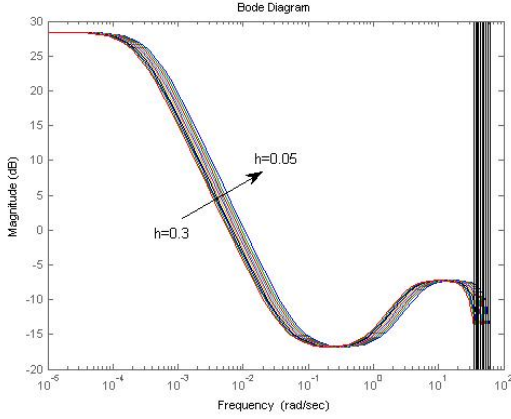


Fig. 7. Bode diagram of the LPV/LFT controller

The sensitivity function  $S$  is presented in Figure 8. The

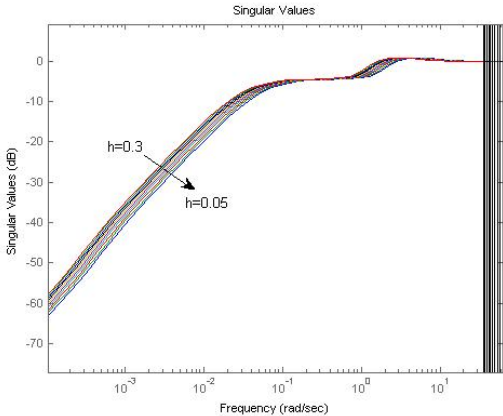


Fig. 8. Sensitivity function

robustness margin is not affected by the sampling period variation, but bandwidth varies. This shows the adaptation of performances w.r.t to current sampling period (because of the varying discrete-time weight on  $\epsilon_z$ ), as required.

## 6. SIMULATION RESULTS

We consider as a mission to follow the sea bottom at constant height and move at constant speed (require for a good interpretation of the results).

The complete linearized model of the AUV is used for the following simulations. We focuses in the sequel on the control of the altitude  $z$ . An independent discrete-time controller control the cruising speed  $u$  which start at 0 and stay constant and equal to  $1m/s$  during all the simulation (its design will not be detailed here; it

is a simple  $\mathcal{H}_\infty$  discrete-time controller, with a sampling period of  $0.1s$ ).

### 6.1 $\mathcal{H}_\infty$ Discrete controller

First, a  $\mathcal{H}_\infty$  controller is synthesized and serves as reference (using *dhinfmi* function of the LMI Control Toolbox). This controller is designed for a single sampling period (not gain scheduled) so could not adapt to sampling period variation. However the robustness brought by the method should allow little variation around  $h = 0.1s$ .

### 6.2 LPV control with sampling period as varying parameter

The controller synthesized in the previous section is used for the control of the system. Different sampling period variation scenarios will be considered, corresponding to different measurement time acquisition.

*Test 1: Constant sampling period* Both controllers are tested on the AUV model, with no variation of the sampling period. The simulation is done with  $h = 0.1s$ , namely the period considered for the  $\mathcal{H}_\infty$  controller design. The LFT controller is adapted to this period via the  $\Delta$  matrix. Simulation results are presented in figure 9.

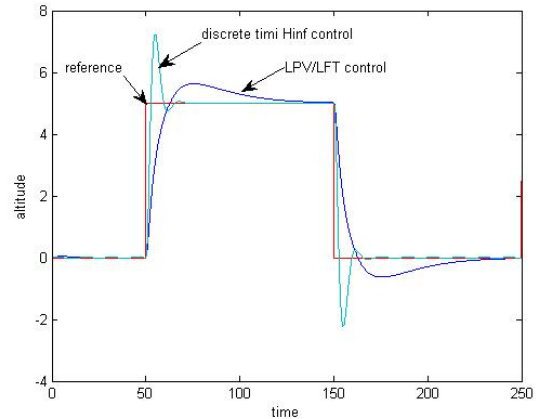


Fig. 9. Test 1: Altitude  $z$  with discrete time  $\mathcal{H}_\infty$  and LFT controllers ( $T_e=0.1s$ )

The  $\mathcal{H}_\infty$  controller gives better results than the LFT one in term of response time but the LFT controller present a smaller overshoot. Both controllers have no tracking error.

*Test 2: Sinusoidal variation of the sampling period  $h$*  For this simulation, the sampling period varies in a sinusoidal way. The step on altitude reference is done at minimal and maximal value of the sampling period, but  $h$  changes (in a sinusoidal way) during the step on  $z$ . Results are presented in Figures 10 and 11.

In the same case the discrete-time controller leads to worst results (in particular for  $h = 0.3$ ) :

The LFT controller gives good results : the system remain stable whatever the sampling period  $h$ . Moreover the adaptation of the performances w.r.t  $h$  is also visible : when the sampling period is high ( $h = h_{max} = 0.3s$ ) the response time is low, and inversely. The discrete-time  $\mathcal{H}_\infty$  controller leads to poor performances especially when

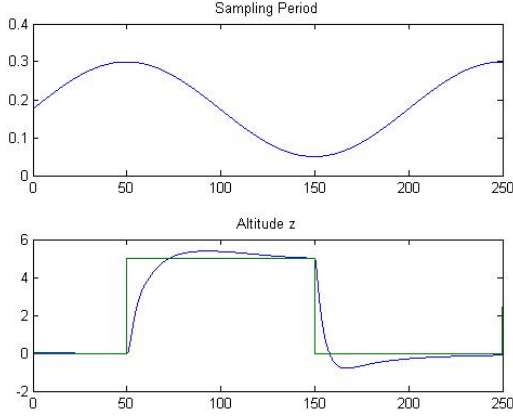


Fig. 10. Test 2: altitude  $z$  with LPV/LFT controller,  $h$  sinusoidal

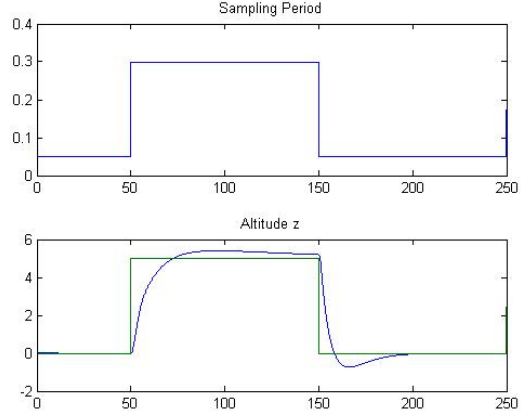


Fig. 12. Test 3: Altitude  $z$  with LPV/LFT controller, step variation of  $h$

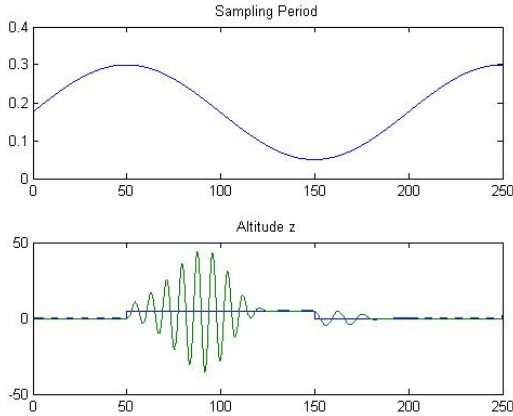


Fig. 11. Test 2: altitude  $z$  with discrete-time  $\mathcal{H}_\infty$  controller,  $h$  sinusoidal

the sampling period is too far from the one used for the synthesis ( $h = 0.3$ ).

*Test 3: Step variation of the sampling period  $h$*  Now we consider two successive step variations of the sampling period on extreme value of the sampling period interval. A step on the altitude reference is done at the same time, to see the influence of the sampling period on the response. Results are presented on Figures 12 and 13.

In the same case the discrete-time controller leads to instability of the system.

The LPV/LFT controller still leads to good results (almost unchanged w.r.t the previous case).

## 7. CONCLUSIONS AND PERSPECTIVES

In this article, we have presented a new formulation for LPV systems, considering the sampling period as varying parameter into an LFT form. During the control design step, the definition of a varying weighting function allows for performance adaptation w.r.t the current sampling period. The main advantage is the robustness of the

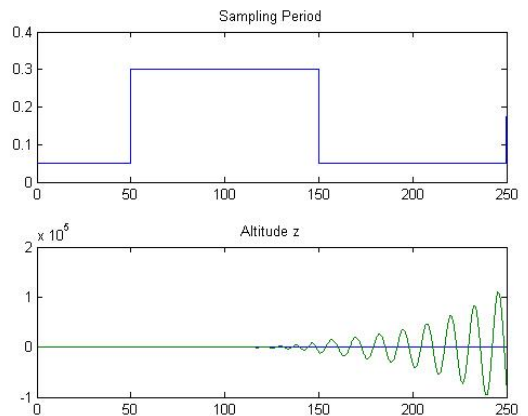


Fig. 13. Test 3: Altitude  $z$  with discrete-time  $\mathcal{H}_\infty$  controller, step variation of  $h$

LPV/LFT method with respect to the variation of the sampling period, considered here as the varying parameter. By adaptation of the controller to the current sampling period, the LFT controller leads to good results whereas the simple discrete-time controller could give instability of the system.

In our work here presented, a unique varying parameter as been considered (the sampling period). In the future, thanks to the LFT formulation, other parameter could be easily added, as for example the forward speed  $u$  (to consider different mission scenarios). In the same way, uncertainties can also be added in the  $\Delta$  matrix.

Finally this controller can be integrated in a global structure of control, to study the interaction between the three decoupled controller in the three dimensions.

## REFERENCES

- Apkarian, P. and Gahinet, P. (1995). A convex characterisation of gain-scheduled  $\mathcal{H}_\infty$  controllers. In *IEEE Transaction on Automatic Control*, volume 40, 853 – 864.



- Feng, Z. and Allen, R. (2004). Reduced order  $\mathcal{H}_\infty$  control of an autonomous underwater vehicle. *Control Engineering Practice : Guidance and control of underwater vehicles*, 12(12), 1511–1520.
- Fossen, T.I. (1994). *Guidance and Control of Ocean Vehicles*. John Wiley & Sons.
- Gauthier, C., Sename, O., Dugard, L., and Meissonnier, G. (2007). An  $\mathcal{H}_\infty$  linear parameter-varying (lpv) controller for a diesel engine common rail injection system. In *Proceedings of the European Control Conference*. Budapest, Hungary.
- Healey, A. and Lienard, D. (1993). Multivariable sliding mode control for autonomous diving and steering of unmanned underwater vehicles. *Oceanic Engineering*, 18(3), 327 – 339.
- Jalving, B. (1994). The NDRE-AUV flight control system. *Oceanic Engineering*, 19(4), 497 – 501.
- Jalving, B. and Storkersen, N. (1994). The control system of an autonomous underwater vehicle. In *Proceedings of the Third IEEE Conference*, volume 2, 851 – 856.
- Lofberg, J. (2004). Yalmip : A toolbox for modeling and optimization in matlab. In *Proceedings of the CACSD Conference*.
- Miyamaoto, S., Aoki, T., Maeda, T., Hirokawa, K., Ichikawa, T., Saitou, T., Kobayashi, H., Kobayashi, E., and Iwasaki, S. (2001). Maneuvering control system design for autonomous underwater vehicle. *MTS/IEEE Conference and Exhibition*, 1, 482 – 489.
- Robert, D. (2007). *Contribution à l'interconnection commande / ordonnancement*. PhD thesis (in french), Institut National Polytechnique de Grenoble.
- Robert, D., Sename, O., and Simon, D. (2010). An  $\mathcal{H}_\infty$  lpv design for sampling varying controllers: Experimentation with a t-inverted pendulum. In *To appear in IEEE Transaction on Control Systems Technology (DOI : 10.1109/TCST.2009.2026179)*.
- Roche, E., Sename, O., and Simon, D. (2009). Lpv /  $\mathcal{H}_\infty$  control of an autonomous underwater vehicle (auv). In *Proceedings of the European Control Conference*. Budapest, Hungary.
- Salgado-Jimenez, T. and Jouvencel, B. (2003). Using a high order sliding modes for diving control a torpedo autonomous underwater vehicle. In *OCEANS*, volume 2, 934 – 939.
- Santos, A.S. (1995). *Contribution à la conception des sous-marins autonomes : architecture des capteurs d'altitude, et commande référencées capteurs*. PhD thesis (in french), Ecole nationale supérieure des Mines de Paris.
- Silvestre, C. and Pascoal, A. (2004). Control of the INFANTE AUV using gain scheduled static output feedback. *Control Engineering Practice*, 12(12), 1501–1509.
- Sturm, J.F. (1999). Using sedumi 1.02, a matlab toolbox for optimization over symmetric cones. *Optimization Methods and Software*, 11-12(1-4), 625–653.